Injection quality of steel cable ducts evaluated by NDT

C.G. Petersen
Germann Instruments A/S, Copenhagen, Denmark

ABSTRACT: Injection of steel cable ducts with grout is important for preventing corrosion on the tensioned strands as well as for stress transfer from the strands to the structural concrete. This paper gives experience obtained from nondestructive testing (NDT) of the grouting quality of steel cable ducts obtained by testing of a controlled specimen containing a fully injected duct with embedded strands and an empty duct. The test systems used are the DOCter Impact-Echo System and the MIRA Ultrasonic-Echo Tomographer. For verification of the test results, the specimen was subsequently examined by cuttings at selected locations. The conclusion is that voided and fully grouted steel ducts can be evaluated by the two NDT systems. Impact-echo can distinguish between reflection from air in the duct and from the steel strands in a fully grouted duct. The ultrasonic-echo tomographer can, with proper color adjustment, also make this distinction. Voids in the grout may be detected by both systems. Verification has to be made by visual inspection of the prestressed strands by opening carefully the ducts without damaging the strands. In an environment with moisture and chlorides it is also necessary to perform chloride analyses of the grout itself and the surrounding concrete.

1 INTRODUCTIO

1.1 *Type area*

During construction of post-tensioned structures strands are inserted into steel cable ducts (Fig. 1) and tensioned (Fig. 2) after the concrete member has achieved sufficient strength. Subsequently, pressure injection of the protective grout takes place from tubes connected to the ducts until the duct has been filled completely with grout, hopefully.

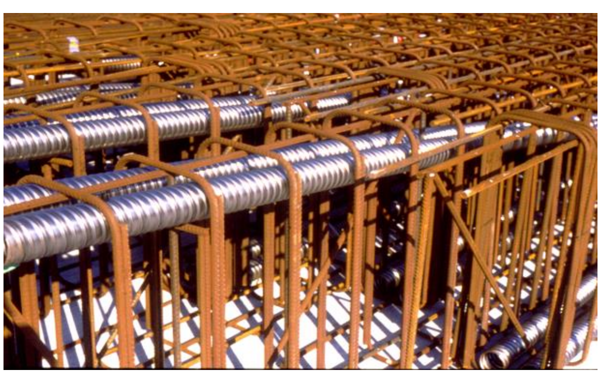

Figure 1 Example of metal ducts.

Figure 2. Post-tensioned strands

The steel ducts, usually about 100 mm in diameter, typically with 10-12 twisted strands, each 15 mm in diameter inserted into them. The depth of the ducts is typically 100 mm to 150 mm in critical areas, depending on the design.

The injected grout has to encapsulate the strands (Fig. 3) to prevent corrosion of the strands (Fig. 4) and to ensure stress transfer from the strands to the structural concrete member. The examples in Figures

3 and 4 are from a post-tensioned bridge beam in Finland constructed in 1971 (Rapaport 2010).

Figure 3. Sound strands in well injected duct

Figure 4. Corroded strands in an empty steel duct.

Consequently, testing for voids in the grout within steel cable ducts is essential, not only at a later stage of a structure's life, but also after setting of the grout for quality assurance purpose.

2 THE NDT METHODS

To minimize destructive invasive testing, selected NDT methods have been used in the past, and are increasingly being used on-site. They are the impact-echo method and the ultrasonic-echo tomographer; both systems are based on stress-wave propagation.

In this paper, experience is given with the two systems for testing on a controlled slab containing voided and fully grouted steel cable ducts 100 mm in diameter. The grouted duct contains 10 twisted strands. The ducts were positioned at ~110 mm depth in a 380-mm thick slab

2.1 *Impact-echo principle (Carino 2015)*

Figure 5 is a schematic of the impact-echo test. A short duration mechanical impact is produced on the concrete surface with a small steel sphere. This impact generates three stress waves, an R-wave on the surface and a P-wave and an S-wave that propagate into the concrete. When the P-wave (the longitudinal wave) and the S-wave (the shear wave) reach a boundary with a material having a different acoustic impedance (wave speed × density), they are reflected and travel back to the surface where the impact was generated. By placing the transducer close to the impact point, the response from the P-wave is maximized, while the S-wave response is minimized. The transducer is a sensitive broadband displacement transducer.

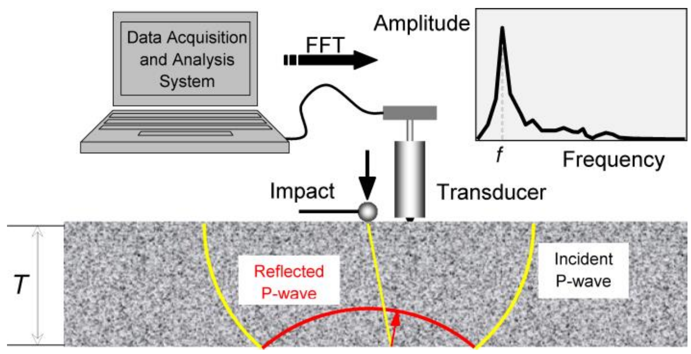

Figure 5. Impact-echo method

Upon reflection at a boundary the P-wave returns into the material and is then reflected back from the surface into the member. The P-wave undergoes, in this manner, multiple reflections between the two surfaces and the recorded waveform of surface displacement has a periodic pattern that is related to the depth of the reflective surface. The displacement waveform is transformed into the frequency domain using the fast Fourier transform (FFT) to produce an amplitude spectrum that shows the predominant frequencies in the waveform.

The analysis of these predominant frequencies is the basis of the impact-echo method, which is governed by the equations shown in Figure 6. The figure shows two conditions (a) a slab with air above and below, and (b) a slab with air above and steel below.

In the first case, the P-wave entering the material will be a compression wave indicated by +. At reflection from a low acoustic impedance surface as air, it will change sign and return to the surface as a tension wave indicated by –. When the tension wave arrives at the surfaces, it causes the surface to move down. At the surface, the P-wave is reflected back into the slab as a compression wave. The process is repeated multiple times. Every time the P-wave arrives at the top surface it will be a tension wave making the surface move downwards. The period in the transducer displacement waveform will be $\Delta t = 2T / C_{plate}$, and the predominant frequency in the amplitude spectrum (not shown) is the inverse of this period.

In the second case, the P-wave enters as a compression wave +. Upon reflection from an interface with a higher acoustic impedance material, such as steel, it will not change sign and returns to the surface as a compression wave +. When the reflected compression wave arrives at the surface, it makes the surface move upwards. The wave then returns as a tension wave –, is reflected against steel as a tension wave –, and makes the surface move down when it arrives at the transducer. This process is repeated. Hence, the period in the transducer displacement waveform will be $\Delta t = 4T / C_{plate}$, and the frequency in the amplitude spectrum (not shown) is the inverse.

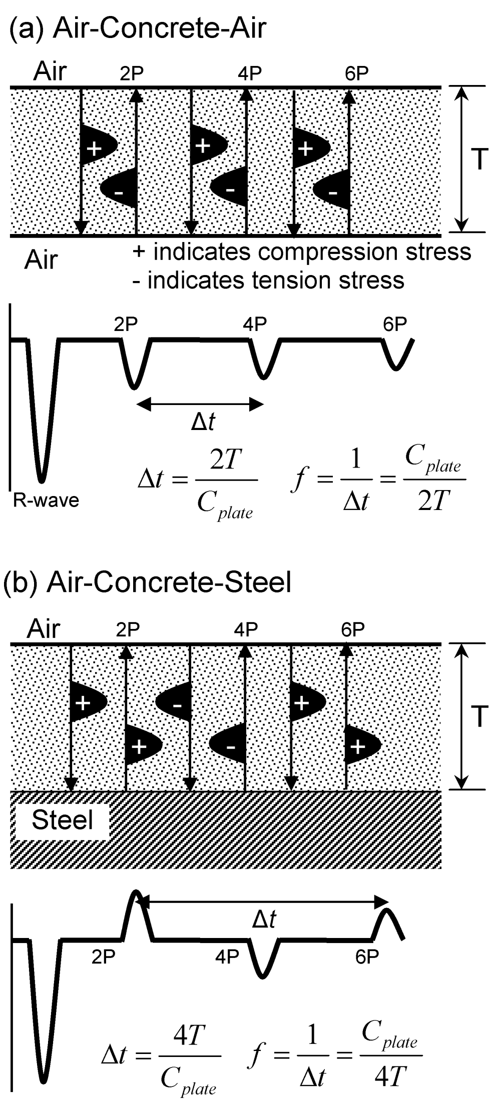

Figure 6. Impact-echo equations for layered systems composed of (a) air-concrete-air and (b) air-concrete-steel (Carino 2015).

As an example, if the P-wave speed in the slab C_{plate} is 4,000 m/s and the thickness T is 200 mm, for the first case, the peak frequency in the amplitude spectrum will be $f = C_{plate}/(2T)$ = 4,000 m/s / (2 × 200 mm) = 10 kHz. For the second case (air-concrete-steel), the frequency will be $f = C_{plate}/(4T)$ = 4,000 m/s / (4 × 200 mm) = 5 kHz.

The information summarized in Figure 6 is of value in being able to distinguish between reflections by air voids in the grout and reflections by the strands surrounded by grout.

2.2 *The ultrasonic-echo tomographer principle (Hoegh et al. 2011)*

Transmitting and receiving transducers are arranged in a "pitch-catch" configuration. One set of transducers sends out a shear wave pulse and all other sets of transducers receive the reflected pulse. The time from the start of the pulse until the arrival of the echo is measured. For a known shear wave speed, C_s, the depth of the reflecting interface can be calculated. The instrument itself measures automatically the shear wave speed.

Figure 7 shows the ultrasonic-echo instrument used in this work. The 4 × 12 transducer array antenna produces many transit time measurements during each test that are analyzed using the synthetic aperture focusing technique (SAFT) in real time to reconstruct a 2D image of the cross section below the instrument. It takes about 3 to 4 seconds to complete data acquisition and data processing at each test location.

Figure 7. The ultrasonic-echo tomographer: (top) top face with display showing 2D cross section image; (bottom) the 4 × 12 transducer array antenna.

Subsequently, the data captured at each test location can be transferred to a computer with dedicated imaging software to create a 3D image of the test region. The software allows views of different slices of the reconstructed internal structure to identify the locations of the reflecting interfaces, which can be the opposite side of the concrete member, reinforcing bars or concrete-air interfaces such as voids, delaminations, honeycombs or other defects.

3 THE TEST SPECIMEN

3.1 *Slab layout*

Figure 8 shows a cross section and plan view of the 400-mm thick slab. One half of the slab was cast on a polystyrene board and the other half was cast against the soil. The slab was 2 m wide in the N-S direction and 3 m long in the E-W direction. A layer of 16-mm reinforcing bars was placed parallel to the short slab dimension with a cover of 40 mm. Two 100-mm diameter corrugated steel ducts, with 1 mm wall thickness, were cast into the east side of the slab. Duct 1 was empty and Duct 2 contained ten 16-mm post-tensioning strands embedded in non-shrink grout as described in 3.2.

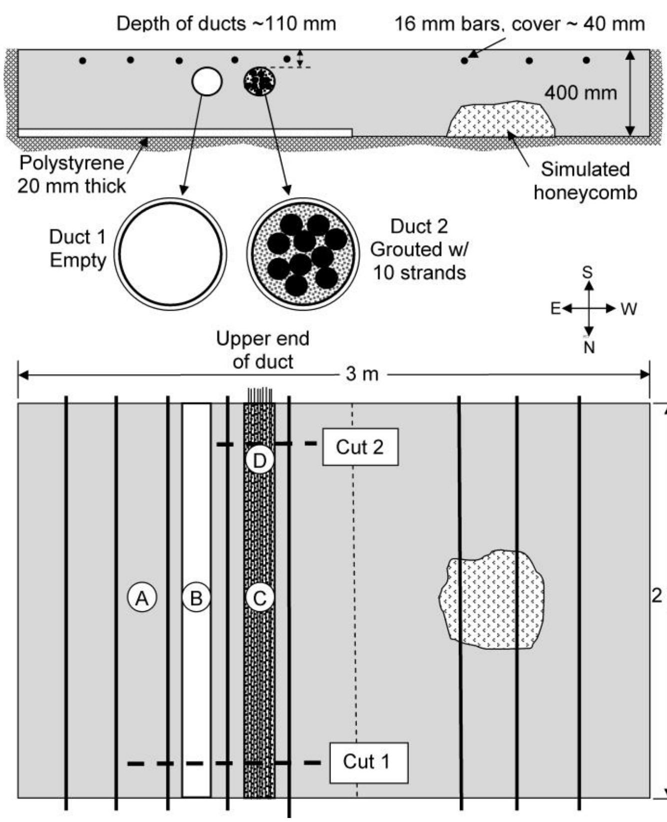

Figure 8. Test specimen

The slab was cast using self-consolidating concrete. Figure 9(a) shows the slab formwork with reinforcement and ducts in place before placing the concrete. Figure 9(b) shows the self-consolidating concrete being pumped into the form.

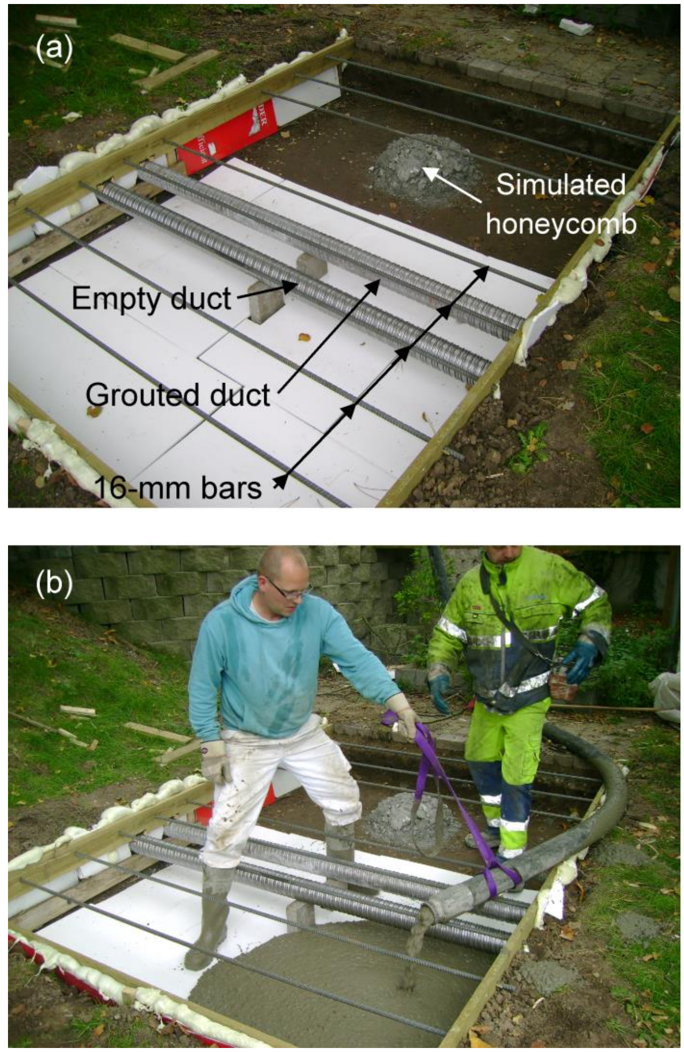

Figure 9. (a) Slab formwork with ducts and bars installed; (b) placing the self-consolidating concrete.

3.2 *Fabrication of the grouted duct with ten strands*

The 2-meter long corrugated steel duct was kept in a fixed vertical position with the bottom resting firmly against a watertight polystyrene plate. BASF MASTERFLOW 9500 grout (with an autogenous shrinkage of 0.1 $^{0}/_{00}$ after 6 days) was mixed in small batches and poured into the duct containing three strands, initially. At a grout height of 200 mm from the bottom, another strand was pushed into the duct, more grout was poured to a height of 400 mm, and another strand was pushed in. The process was repeated until all ten strands were positioned in the duct surrounded by grout to the top. Constantly during casting, the grout was externally vibrated by gently tapping the duct with a rubber mallet to ensure total embedment of the strands in the grout. While filling the upper end of the duct, about 200 mm from the top, the mixer broke down, and another less efficient mixer had to be used.

The cable duct was kept in the same vertical position for 30 days and then placed carefully in the slab formwork (Fig. 9(a)). The upper end of the duct was positioned on the "south" side of the slab, with the strands sticking out of the slab as shown in Figure 8.

4 TESTING

4.1 *Impact-echo*

The impact-echo equipment used is shown in Figure. 10.

The plate P-wave speed C_{plate} was determined by thickness measurement and an impact-echo test of the solid slab. For a thickness of 380 mm (slab on polystyrene board) and a measured frequency of 5.37 kHz, the P-wave speed is $C_{plate} = f \times 2 \times \mathrm{T} = 5.37$ kHz × 2 × 380 mm = 4081 m/s, which is quite reasonable for good quality concrete.

For a void at 110 mm depth, the expected frequency will be $f = C_{plate} /(2{\times}T_v)$ = 4081 m/s / (2 ×110 mm) = 18.55 kHz, and for a steel interface (the strands) at about 115 mm depth, the expected frequency is $f = C_{plate} /(4{\times}T_s)$ = 4081 m/s / (4 × 115 mm) = 8.87 kHz.

Testing took place along the centerlines of the ducts at a spacing of 50 mm with the impactor positioned 10 to 20 mm from the transducer tip along the centerline of the duct. The selected impactor was primarily an 8-mm steel ball producing a maximum useful frequency of ~20 kHz and, secondarily, a 5-mm impactor with a maximum useful frequency of ~40 kHz (see Carino 2015).

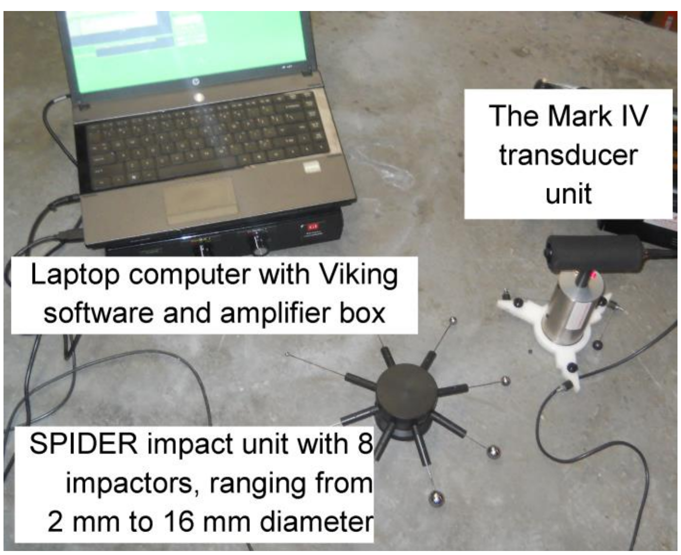

Figure 10. The impact-echo test equipment used

The test results were classified into four categories as follows (see Fig. 8):

1. Category A, solid slab
2. Category B, empty cable duct (40 test results)
3. Category C, fully grouted duct (34 test results)
4. Category D, poorly grouted duct (6 test results)

4.1.1 *Category A—solid slab*

Figure 11 is an example of a test result for the solid slab. The upper window shows the transducer displacement signal in the time domain. The lower window shows the amplitude spectrum, which indicates the frequencies contained in the transducer displacement signal. Two boxes are shown in the upper right hand corner of the amplitude spectrum: an upper box (in red) displaying a frequency and a calculated depth and a lower box (in blue) showing the expected frequency for a solid slab.

For a slab thickness of 380 mm and a plate P-wave speed is 4081 m/s, the expected solid frequency is 5.37 kHz, following the impact-echo equation for air-concrete-air (Fig. 6). This frequency is shown in the lower (blue) box in the amplitude spectrum window. The measured frequency in the upper red box, 5.37 kHz, coincides with this expected frequency and the calculated thickness of 380 mm corresponds to the slab thickness. Thus the test indicates a solid slab. The amplitude spectrum displays two cursors (vertical lines) that correspond to the frequencies shown in the upper and lower boxes: a blue cursor positioned at the expected frequency for a solid slab and a red cursor positioned at the peak frequency. In Figure 11, the red cursor related to the measured frequency shown in the top (red) box is hidden behind the blue cursor. This red cursor will be positioned automatically at the highest peak, but it can be moved manually to other peaks in the spectrum, and the red box will show the depth corresponding to that frequency.

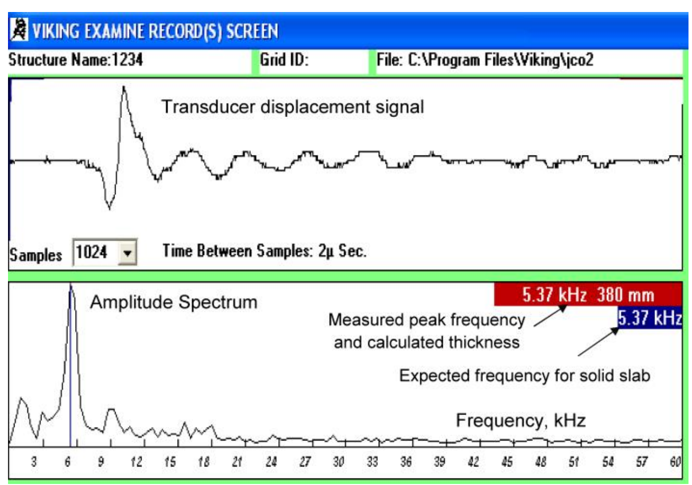

Figure 11. Impact-echo result for solid slab

4.1.2 *Category B—empty duct*

Figure 12 shows a result from a test at a point above the empty duct. The 5.37 kHz solid plate frequency peak in Figure11 has dropped to a lower value of 4.39 kHz, meaning that the apparent travel path of the P-wave is: (4081 m/s / (2 × 4.39 kHz)) = 464 mm, 84 mm longer than 380 mm for the solid plate. Consequently, the P-wave is travelling around the reflection surface, which is the empty cable duct. At the same time, a frequency peak at 19.51 kHz shows up, where the red cursor is positioned. This frequency relates to a depth to the reflection surface of 105 mm, the depth of the empty cable duct indicated in the red box. A 5mm impactor was used to accentuate the high frequency peak.

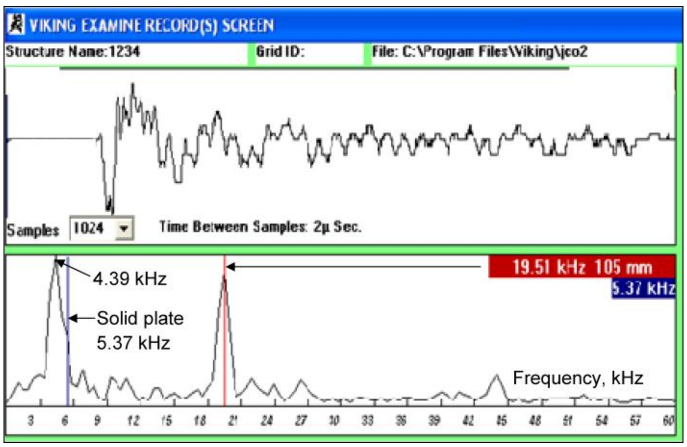

Figure 12. Impact-echo result above empty duct

4.1.3 *Category C—fully grouted duct*

Figure 13 shows the result for a test at a point over the fully grouted duct. The 5.37 kHz frequency measured is the same as the solid frequency in Figure 11, indicating a P-wave travel path of 380 mm. This can only happen if the duct with the strands is fully grouted with no air intrusions, provided the testing is made over the duct. To make sure this is the case, there has to be an additional reflection from the strands inside the grouted duct. This reflection shows up as a peak at 9.27 kHz, equivalent to a depth to the steel strands of T_s = 4081 m/s / (4 × 9.27 kHz) = 110 mm (half of the 220 mm indicated in the red box), based on the impact-echo equation for air-concrete-steel as shown in Figure 6. An 8 mm impactor was used.

4.1.4 *Category D—poorly grouted duct*

Fig. 14 shows the result for another test at a point above the grouted duct. The P-wave has a travel path of more than 380 mm as the frequency has dropped from 5.37 kHz to 4.80 kHz. This can only happen if there is air in the duct. The air interface is positioned at a depth of 107 mm as indicated by the peak at a frequency of 19.02 kHz. The interpretation is that the duct is poorly grouted and has air voids. An 8 mm impactor was used.

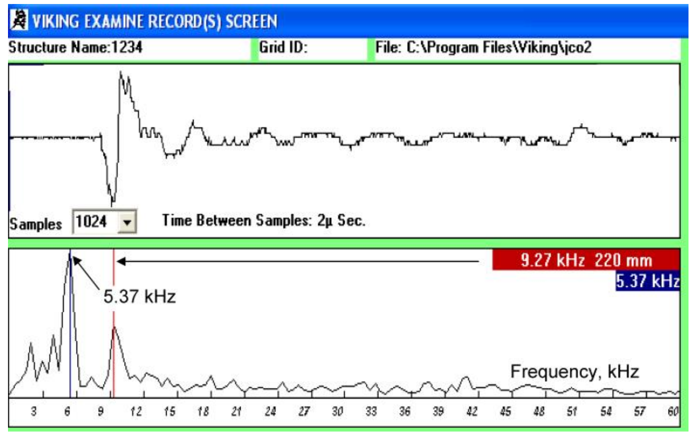

Figure 13. Impact-echo result over fully grouted duct.

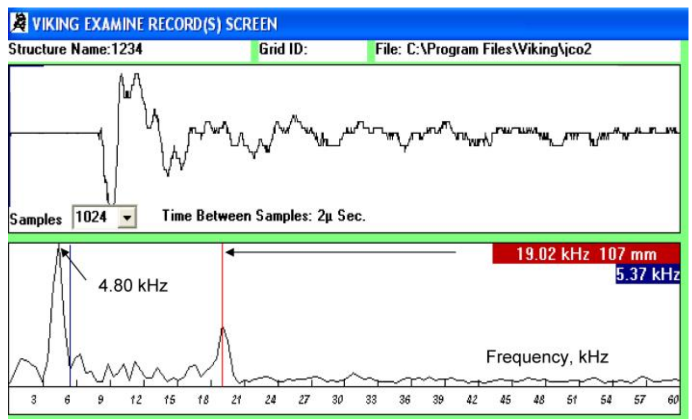

Figure 14. Impact-echo result due to voids in grout

4.2 *Ultrasonic-echo tomographer*

As shown in Figure 15, testing was done along two scan lines above the ducts with 250 mm distance between the scan lines and in steps of 100 mm, going from South to North along the 2 meter wide slab.

The settings of the ultrasonic-echo tomographer were:

- Operating frequency: 25 kHz
- Color option: MIRA
- Color gain: 7 dB
- Analog gain: 30 dB

After transferring the records into the *IdealViewer* software, various images were examined as shown in Figures 16 to 20.

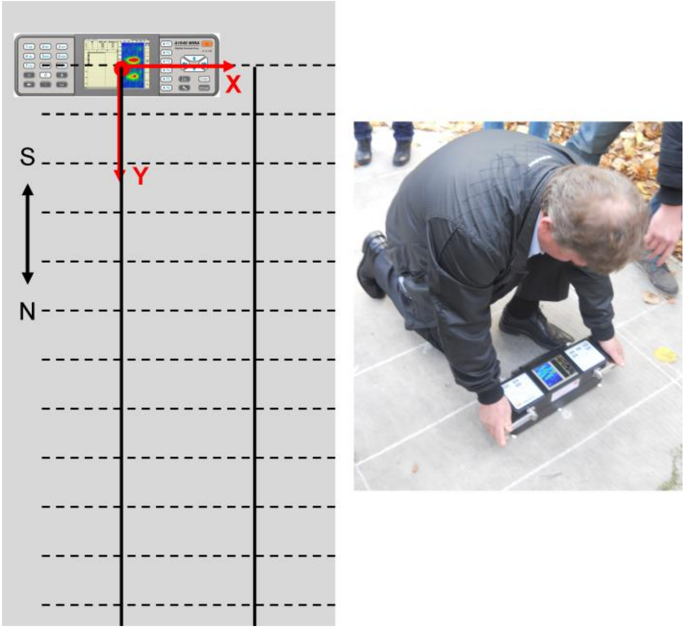

Figure 15. Testing above cable ducts with ultrasonic-echo to-mographer

Figure 16 is a 3-D color image of the volume around the ducts. The volume has been clipped so that the back-wall reflection is not shown. The two ducts and the reinforcement bar located between the center lines of the ducts are clearly visible. Note that the south end of the grouted duct shows the same red color as for the empty duct.

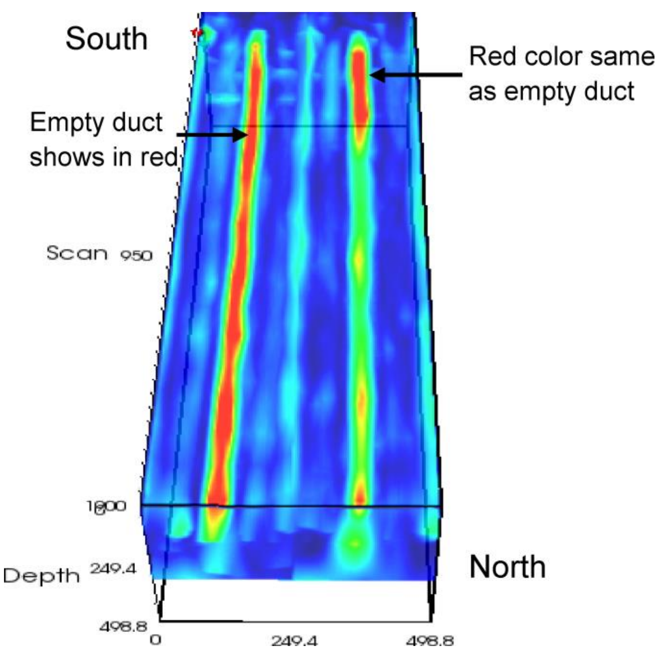

Figure 16.3D color image of volume tested in vicinity of ducts.

Figure 17 shows a side view of the empty duct (D-Scan). The reflection from the bottom of the slab (back wall) is seen clearly. The empty duct is displayed in red color.

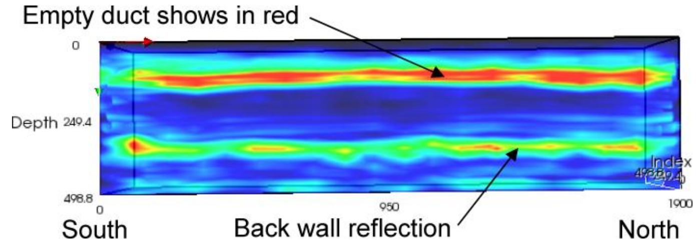

Figure 17. Side view (D-scan) of the reflections from the empty duct and bottom of slab.

Figure 18 is a side view of the grouted duct. Note the red color near the south end of the duct.

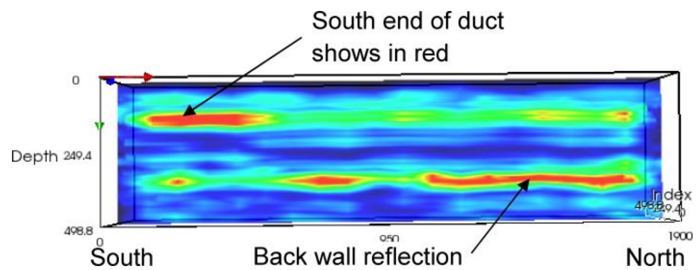

Figure 18. Side view (D-scan) of the reflection from the grout-ed duct and bottom of slab.

Figure 19 shows and end view (B-Scan) of the slab and ducts at a plane 1200 mm from the south face. Reflections from the reinforcing bars can be seen. Reflections from the empty duct show in red, reflections from the grouted duct show in a blue-green color, and the bottom of the slab is seen clear-ly.

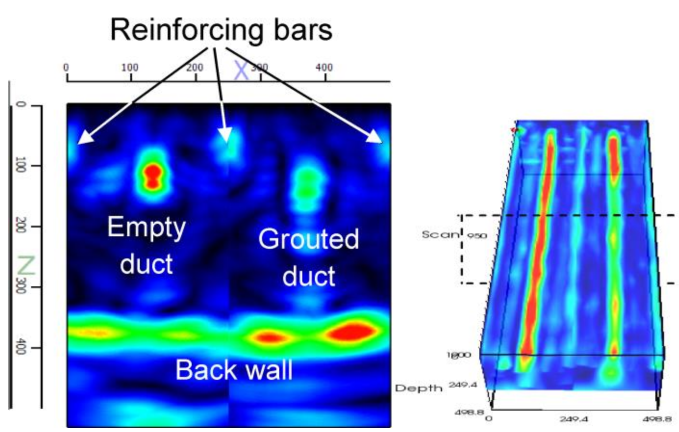

Figure 19. End view (B-scan) at cross section 1.2 m from south face

Figure 20 shows an end view of the slab and ducts at a plane 150 mm from the south face. The similarity in the red colors of the images representing the two ducts indicates that the grouted duct is in fact not fully grouted. Starting from the south face of the specimen and extending about 200 mm along the duct, the red reflection indicates air voids are present in the duct (see also Figs. 16 and 17).

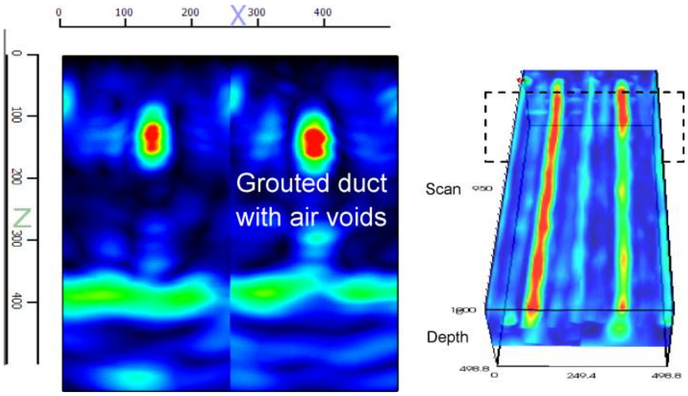

Figure 20. End view (B-scan) at cross section 150 mm from south face.

5 CUTTING SLAB FOR VERIFICATION

The slab was cut at two positions as shown in Figure 8 to verify the interpretations of the impact-echo and ultrasonic-echo test results. Cut 1 was made near the north face, where test results indicated the grouted duct did not have voids in the grout. Figure 21 shows that, in fact, there were no voids in the grout.

Figure 21. Cut 1 for verification that duct with the 10 strands was fully grouted.

Cut 2 was made near the south face as shown in Figure 8. This location was classified as poorly grouted. As shown in Figure 22 there were, in fact, large air voids in the grout, which have been colored black in the photo for better contrast.

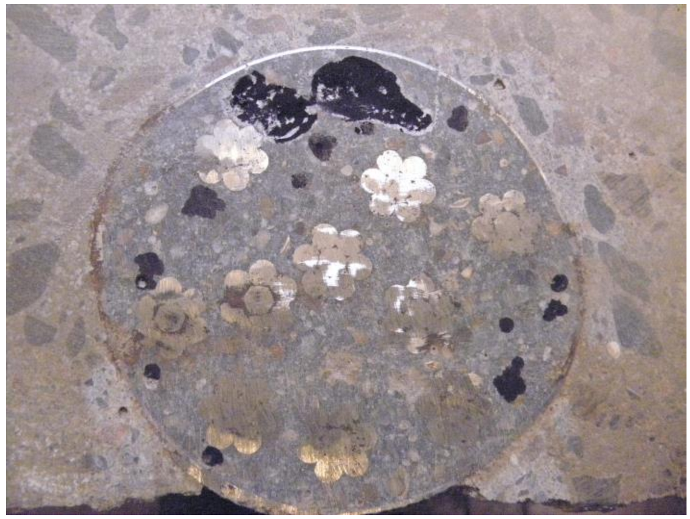

Figure 22. Cut 2 for verification of voids in grouted duct; air voids are enhanced by black marking.

Thus the test results were confirmed, and the grouted duct had unplanned voids, which were likely a result of the problems encountered when the last part of the duct was filled with grout.

6 CONCLUSIONS

Both the impact-echo method and the ultrasonic-echo tomographer can detect steel cable ducts without grout.

For practical testing with impact-echo, it is important to test along the longitudinal axis of the duct. Prior to testing, the duct(s) have to be located e.g. by GPR, a deep cover meter, or by the ultrasonic-echo tomographer. During testing, make sure a reflection frequency is obtained from either the strands in the duct with no drop in the solid frequency, or from a void in the duct accompanied by a drop in the solid frequency. Should the concrete member have changing thickness, the only practical approach is to look for either the frequency associated with reflection from the strands in the grouted duct, or the frequency associated with reflections from voids in the grout.

The ultrasonic-echo tomographer needs adjustment of the image colors for detection of cable ducts without grout.

Partly grouted steel cable ducts can also be detected with both systems. Care should, however, be exercised in interpreting the results. In spite of the presence of voids in the grout the strands may be fully protected and well bonded to the grout. Only invasive opening will reveal the actual condition of a partially grouted steel cable duct.

Detection of fully grouted steel cable ducts with the ultrasonic-echo tomographer will require proper adjustment of the image colors. For the impact-echo method, the frequency associated with reflections from the strands will be in accord with following the equation $f = C_{plate} / (4 \times T_s)$ with no drop in the solid plate frequency.

Verification of the NDT testing results by invasive probing should be done carefully to prevent damaging the prestressing steel. An additional advantage of the verification (opening of the duct) is that evaluation can be made of the degree of corrosion of the prestressing steel. Samples of the injection grout should be taken for chloride analysis to determine if chlorides have penetrated into the duct, for example from a leaking expansion joint or from corroding regions on the steel cable duct.

As an example, Ramboll Finland Oy (Rapaport 2010) has already applied successfully this kind of testing on more than 50 bridges and has gathered a lot of experience in these types of investigations. One of the important conclusions is that in order to be able to correctly interpret the test results the testing engineer needs to have a lot of experience and understanding of the systems and of the construction of the tested structures.

REFERENCES

Rapaport, Guy: “Scanning by MIRA 3D Tomographer, Test Case, Lieviö Overbridge, Finland”, Ramboll, Kuipio, Finland, 24.10.2010

Carino, N.J.: “Impact Echo: The Fundamentals”, International Symposium on Non-Destructive Testing in Civil Engineering, September 15-17, 2015, Berlin, Germany http://www.ndt.net/article/ndtce2015/papers/257_carino_nicholas.pdf

Hoegh K., Khazanovich L., Yu H.T. “Ultrasonic Tomography Technique for Evaluation of Concrete Pavements.” *Transportation Research Record*: *Journal of the Transportation, Research Board*, No. 2232, pp. 85–94. 2011, Washington, USA